

KfK 3021
August 1980

Laboratory Studies of the Meltfront Propagation in a Borax Core-Catcher

M. Dalle Donne, H. Werle
Institut für Neutronenphysik und Reaktortechnik
Projekt Schneller Brüter

Kernforschungszentrum Karlsruhe

KERNFORSCHUNGSZENTRUM KARLSRUHE

Institut für Neutronenphysik und Reaktortechnik

Projekt Schneller Brüter

KfK 3021

Laboratory Studies of the Meltfront Propagation
in a Borax Core-Catcher

M. Dalle Donne and H. Werle

Kernforschungszentrum Karlsruhe GmbH, Karlsruhe

Als Manuskript vervielfältigt
Für diesen Bericht behalten wir uns alle Rechte vor

Kernforschungszentrum Karlsruhe GmbH

Abstract

A series of seven laboratory experiments concerning the meltdown of a borax core-catcher have been performed. By the selection of the simulant materials the most important thermophysical properties of the core-catcher materials were taken into account. Fission - product heating of the molten core masses was simulated by electrolytically heating of the molten region. The experiments reveal interesting details of the phenomena to be expected during melt-down of a borax core-catcher , especially on the flow pattern, the mixing processes of molten materials and the layer formation in the melt. The most interesting result is that the ratio of downward to sideward melting rate is heavily reduced by high melting barriers and that a cubic structure of barriers will not equalize downward and sideward melting rates. A Super 8 film is available as additional information.

Kurzfassung

Modellexperimente zur Schmelzfront-Ausbreitung in einem Borax-Kernfänger

Es wurde eine Reihe von sieben Modellexperimenten zum transienten Abschmelzverhalten eines Borax-Kernfängers durchgeführt. Die Simulationsmaterialien wurden unter Berücksichtigung der wichtigsten, thermophysikalischen Eigenschaften der Kernfänger-Materialien aus- gesucht. Die Beheizung der Kernschmelze durch die Spaltprodukte wurde durch elektrolytische Beheizung des aufgeschmolzenen Bereichs simuliert. Die Experimente geben Aufschluß über die während des Abschmelzens eines Borax-Kernfängers zu erwartenden Phänomene, ins- besondere über das Strömungsbild, die Vermischungsvorgänge der aufgeschmolzenen Materialien und Schichtenbildung in der Schmelze. Das interessanteste Ergebnis ist, daß das Verhältnis der vertikalen und radialen Abschmelzrate durch hochschmelzende Barrieren drastisch reduziert wird und daß eine kubische Barrierenstruktur nicht dazu führt, daß die vertikale und radiale Abschmelzrate gleich werden. Als zusätzliche Dokumentation steht ein Super 8-Film zur Verfügung.

1. Introduction

Core-catchers for gas and sodium cooled fast reactors using sodium borates as sacrificial material have been proposed /1/. UO_2 , PuO_2 and the fission product oxides are dissolved by the sodium borates, provided they remain in contact for a sufficiently long time at sufficiently high temperatures. The core-catcher for a (1000 MW_e) gas-cooled fast reactor is based upon borax ($\text{Na}_2 \text{B}_4 \text{O}_7$). The borax is contained in steel boxes forming a 2.2 m thick slab on the base of the reactor cavity inside the prestressed concrete reactor vessel, just underneath the core (Fig. 1) /2/.

Material related questions, like solubility of UO_2 in borax, borax evaporation rate, compatibility between graphite and borax at high temperatures, have been studied in laboratory tests /1-3/. As far as the thermohydraulic behaviour is concerned, two phases may be distinguished:

An instationary phase beginning when the molten core masses enter the core-catcher and ending when the slab of borax filled steel boxes is completely molten and a quasistationary phase afterwards. In the quasistationary phase the oxydic fission products are dispersed in the pool formed by liquid borax and the metallic fission products are contained in the steel lying below the borax pool (Fig. 1).

Natural convection heat transfer for a volume-heated, cylindrical pool has been studied experimentally /4,5/, and the results confirm the semiempirical model of Baker et al. /6/. Using this model the thermal behaviour of core-catchers for gas- and sodium-cooled fast reactors in the quasistationary phase has been analyzed /1/, with the result that both, the pool temperatures as well as the heat fluxes to the liner, are sufficiently low.

Whereas there exists sufficient knowledge to predict the thermal behaviour after the sacrificial material has been molten and a quasistationary pool within fixed boundaries has developed, very little is known about the behaviour of a growing pool in the preceding, instationary phase. A certain knowledge of the instationary phase is necessary for two reasons:

Firstly, the final state of the transient phase has to be known, because this determines the boundary conditions for the quasistationary phase. In addition, also in the transient phase, the local heat flux to the liner must not exceed certain limits, which could happen, if the melt velocities downward and sideward would be very different.

From experimental studies of pool growth in solid, soluble materials [7-9], it is known, that the ratio of downward to sideward melting rate depends strongly on the liquid to solid density ratio ρ^* . Downward to sideward penetration is < 1 , ≈ 1 , ≈ 2 for $\rho^* < 1$, ≈ 1.5 and 4, respectively. Therefore, it is to be expected, that in a catcher consisting of borax (density 2.4 g/cm³) only, the molten core masses would penetrate mainly downward. For construction purposes and to provide high melting barriers to the downward movement of the fuel the borax is contained in steel boxes (Fig. 1). These barriers should guarantee that the fuel and borax remain in contact for a sufficient time at sufficiently high temperatures. In addition, it was assumed [1,2], that the cubic steel containers would lead to equal penetration velocities in radial and vertical direction.

Laboratory experiments were performed to study pool growth in a core-catcher consisting of a soluble, sacrificial material in between high melting barriers. The goal of these experiments were twofold: Firstly they were aimed at getting a picture of the processes occurring during the meltdown of such a device and secondly, more specific, to study the influence of high melting barriers. It is very difficult to prove thermohydraulic similarity for this complicated geometry, thus the application of the results to the reactor situation is subject to some reservations.

2. Experiments

2.1 Similarity considerations

The growth of the liquid pool consisting of fuel and dissolved sacrificial material in a borax core-catcher depends on the

- thermophysical properties of the materials involved
- heating mode
- geometry
- initial and boundary conditions.

As far as the thermophysical properties are concerned the following seem especially important:

- fuel is soluble in borax
- fuel is considerably heavier than borax
- steel is heavier than the fuel-borax mixture
- melting point of steel is higher than that of borax.

With the choice of a concentrated, aqueous solution of $ZnBr_2$ (density 1.83 g/cm^3) for the molten fuel, of polyethylene glycol 1500 (PEG, density 1.10 g/cm^3 , melting point 44°C) for borax and Wood metal (density 9.5 g/cm^3 , melting point 70°C) for steel, these material requirements are, at least qualitatively, correctly reproduced. The melted PEG is miscible with aqueous solutions.

In the core-catcher, the molten region is volume-heated by the dissolved fission products. This seems to be sufficiently well simulated in the experiments by heating the liquid pool electrolytically.

The borax core-catcher has a cylindrical geometry. In the experiments, a two-dimensional (x-z) arrangement, which corresponds to a slide of the original cylinder, has been used. In the second horizontal direction (y) the meltfront propagation is prevented by the container walls. The volume ratio of steel to borax (2 %) could not be well reproduced in the experiments (6-12 %).

As initial conditions it was assumed that the molten core masses are located in the upper, central region of the core-catcher. In the experiments the boundaries, except the upper, are essentially adiabatic. This seems a good simulation of the conditions in the core-catcher as long as the meltfront has not reached the cooled liner wall.

In summarizing, it seems, that the characteristics of the borax core-catcher can be simulated quite well in the experiments.

2.2 Experimental set-up and procedure

Seven experiments were performed altogether. They are numbered chronologically (BORAX-1 to 7). Details are given in table 1.

BORAX-7 (Fig.2) constitutes the reference experiment. The sacrificial bed consists of pure polyethylene glycol 1500 (PEG) without any Wood metal structure. The overall dimensions are: Width 22 cm, height 17 cm, depth 5 cm. The empty space (width 12 cm, height 12 cm, depth 5 cm) in the piece of PEG is filled at the beginning of the experiment with $\text{H}_2\text{O-ZnBr}_2$, which simulates the molten core masses. The density of $\text{H}_2\text{O-ZnBr}_2$ was 1.83 g/cm^3 at 44°C (melting point of PEG), and this value was used in most other experiments. The liquid region is heated by passing a 50 Hz current between two vertical screen electrodes located at the front and the back, respectively. The whole arrangement is contained in a lucite container (wall thickness 1 cm) and corresponds to one half of a slide cut from the cylindrical core-catcher, with the axis at the right boundary of the container. The experiment is instrumented with four thermocouples which are periodically recorded. After pouring the $\text{H}_2\text{O-ZnBr}_2$, electrical power is supplied to the electrodes. The meltfront propagation downward and sideward is observed optically by a camera, taking pictures at intervals of some minutes and by a Super 8 film camera (2-5 s/frame).

In BORAX-4 to 6 (Fig. 3-7) the geometry and dimensions are the same as in BORAX-7. The sacrificial bed consists of a cubic structure (pitch width 1 cm) of Wood metal (wall thickness 0.35 mm) filled with PEG or PEG + $\text{H}_2\text{O-KJ}$ (BORAX-6). The cubic structure simulates the steel boxes.

The wall thickness of the equivalent boxes would amount to $0.35 \text{ mm}/2 = 0.175 \text{ mm}$. The metallic structure would cause a short circuit if inserted between the vertical screen electrodes. Therefore, for BORAX-4 to 6 and also for BORAX-2 and 3 electrolytical heating was applied by using an electrode located in the empty space of the sacrificial bed and the Wood metal structure as second electrode (Fig. 3). The shape of the electrode can be changed during the experiment. In this way it is possible to get an approximately uniform distance between the electrodes and thereby an uniform volumetric power density in the liquid pool. In Borax-6, in contrast to all other experiments, the Wood metal structure was filled with a mixture of $\text{H}_2\text{O-KJ}$ ($\rho = 1.67 \text{ g/cm}^3$) and PEG (vol. fraction ratio 2:15). The density of the mixture was about 1.19 g/cm^3 , the melting point 25°C and the electrical conductivity about 70 % of that for $\text{H}_2\text{O-ZnBr}_2$. The reason for adding $\text{H}_2\text{O-KJ}$ to the PEG in this experiment was the observation, that the sacrificial material and the initial pool do not mix completely. Layers with different concentrations may exist and this might lead to nonuniform power densities if the electrical resistance of the two components is very different. In BORAX-5 the density of the initial melt was only 1.22 g/cm^3 . The results of BORAX-5 together with those of BORAX-4 and 6 should therefore allow some extrapolation to the yet higher density ratio of a borax core-catcher (density ratio $\text{UO}_2/\text{borax} \approx 9/2.4$).

The series of experiments BORAX-1 to 3 (Fig. 8-14) differ in some important aspects from the series BORAX-4 to 7. Firstly, a whole slide of the cylindrical core-catcher is simulated, i.e. the axis corresponds to the center of the experimental arrangement. The empty space (width 15 cm, height 5 cm, depth 10 cm) is correspondingly located in the central region of the sacrificial bed and the overall dimensions (width 36 cm, height 15 cm, depth 10 cm) are larger. Secondly, the sacrificial bed is made up of real cubic boxes (5cm · 5cm · 5cm). The wall thickness of the boxes was 1 mm for BORAX-1 and 2 and 0.5 mm for BORAX-3. In BORAX-1 and 2 the density of the initial melt was again 1.83 g/cm^3 as for most other experiments. In BORAX-4 the melt density was reduced to 1.19 g/cm^3 for the same reason as discussed for BORAX-5. Whereas in all other experiments the liquid pool was electrolytically heated, in BORAX-1 the empty space in the sacrificial bed was heated by a fixed arrangement of 28 wires, electrically heated and running in

parallel from the front to the back of the container. This heating method is not a good simulation of the fission-product heating, especially because the heated region does not move with the meltfront. Comparisons with the other experiments should give some information on the sensitivity of the results against changes in the heating mode.

The power, 150 or 200 W, was normally kept constant during one experiment. In some cases, the power was raised to a higher value in a later stage of an experiment to accelerate the meltfront propagation.

3. Discussion of results

3.1 Downward to sideward meltfront propagation

Intolerable high liner heat fluxes could arise temporarily in the borax core-catcher if the downward and sideward meltfront propagation velocities are very different. The downward to sideward meltfront velocity ratio is therefore the most interesting quantity in these experiments.

For the series of experiments BORAX-4 to 7 the meltfront propagation is shown in Fig. 2 to 5, the temperatures of the three thermocouples located in the pool and the power history in Fig. 6. In Fig. 7 the sideward and downward penetration of both meltfronts, that for PEG and that for the Wood metal structure, are shown as a function of time. The PEG meltfront is visible in Fig. 2 to 5, because there is a thin layer of PEG between the Wood metal structure and the container wall. Initially, the meltfronts propagate approximately linearly with time. The corresponding, initial meltfront velocities are given in the following table:

Initial meltfront velocities (cm/min)

	Downward		Sideward		Downward/Sideward	
	PEG	Wood	PEG	Wood	PEG	Wood
BORAX-4	.10	.080	.24	.26	.42	.31
5	.080	.018	.22	.23	.36	.08
6	.17	.12	.31	.35	.55	.34
7	.26	----	.21	---	1.24	---

Compared to BORAX-7, the initial downward to sideward PEG meltfront velocity ratios in BORAX-4 and 6, which we think are the best simulations of the borax core-catcher, are only 34 and 44 %, respectively. Moreover, in BORAX-4 and 6 downward propagation of the Wood metal meltfront decreases strongly after about 3 cm of the sacrificial bed have been molten (Probably due to the formation of a liquid Wood metal layer). Compared to BORAX-4, the downward propagation in BORAX-6, where the Wood metal structure has been filled with PEG + H₂O-KJ to avoid inhomogeneities in the power density, is only slightly higher. From this we conclude, that any power density inhomogeneities in the experiments with pure PEG have only a minor influence on the meltfront propagation. BORAX-5 demonstrates the strong influence of the pool to sacrificial material density ratio on the downward to sideward meltfront velocity ratio. Especially the downward meltfront velocity of the Wood metal structure is in BORAX-5 much smaller (about a factor 5) than in BORAX-4 and 6. The local heat fluxes are inversely proportional to the distances between the PEG and Wood metal meltfront. Using these distances, the initial downward to sideward heat flux ratios are estimated to be about 0.5, 0.3 and 0.6 for BORAX-4, 5 and 6, respectively. These values are in accordance with the meltfront velocity ratios given in the table above.

The series of experiments BORAX-1 to 3 are certainly inferior to the series BORAX-4 to 6, especially because the dimension of the Wood metal boxes are not sufficiently small compared to the overall dimensions and to the distance between the two electrodes (2 cm) (giving rise to power density inhomogeneities). Nevertheless, by comparing the two series one might get an impression on the sensitivity of the results to changes in the structure of the sacrificial layer. The meltfront propagation is shown in Fig. 8 to 10, temperatures and power histories in Fig. 11 to 13. The meltfront of the Wood metal structure as a function of time is shown in Fig. 14. Similar as for the series BORAX-4 to 6, this figure shows, that the sideward meltfront propagates continuously up to the container wall, whereas downward propagations stops after only a fraction of the first lower row of boxes has been molten. In accordance with BORAX-5 the vertical propagation of the low density pool in BORAX-3 is very slow.

The following conclusions may be drawn from these results:

- By the insertion of high melting barriers in a sacrificial bed the ratio of downward to sideward meltfront propagation can be reduced until nearly zero. Downward and sideward propagation is not equal as has been tentatively assumed for a cubic structure of barriers in /1,2/.
- As is the case with homogenous sacrificial layers /7-9/, the ratio of downward to sideward propagation increases strongly with increasing pool to sacrificial material density ratio.
- Substantial changes in the local power density distribution and in the structure of the sacrificial bed have only minor influences on the meltfront propagation. Therefore, the experimental results seem to be reliable and the application to the borax core-catcher justified.

3.2 Special effects

From the photographs of the meltfront propagation one gets a good idea how a borax core-catcher may behave during the transient phase. In addition some interesting phenomena have been observed in the experiments.

Firstly, due to the finite solution velocity, the pool may consist, as is shown for BORAX-2 in Fig. 15, of three layers: At the top there is pure PEG, at the bottom $H_2O-ZnBr_2$ with some PEG and in the central region PEG with a little amount of $H_2O-ZnBr_2$. In some of the photographs of the meltfront these layers are clearly visible. This layer configuration is especially pronounced in the experiments with high initial liquid density. The observation of these layers was the reason why in the BORAX-6 experiment the Wood metal structure was filled with PEG + H_2O-KJ instead with pure PEG (to avoid an inhomogeneous power density). In BORAX-6 too, layers have been observed. But it has been checked by measuring vertical temperature profiles in the lower layer and near the boundary between the lower and central layer that the lower layer is nearly (within $5^\circ C$) isothermal. The uniform temperature in the lower layer is attributed

to convective movement due to volume heating, because at the time of measuring (15h30, see Fig. 5-2) there was no longer any agitation by upward streaming PEG. It should be mentioned, that a similar layer configuration is conceivable also in a borax core-catcher.

Whereas with a high density of the liquid, the mixing process with the molten PEG is very turbulent, with a low density liquid the molten PEG rises in "Schlieren" through the liquid (Fig. 4-3). These "Schlieren" are very stable with lifetimes up to some ten minutes.

4. Conclusions

From these series of seven BORAX experiments one gets a good idea on the phenomena occurring during meltdown of the sacrificial bed caused by the fission-product heated fuel pool in a borax core-catcher. The photographic recording reveals interesting details on the

- movement of sacrificial and barriers material
- flow pattern, mixing processes and layer structures in the pool.

The most interesting result is the ratio of downward to sideward propagation and, more specifically, the change of this quantity when a bed of pure sacrificial material is replaced by one, where, the same sacrificial material is contained within a structure of high melting barriers. At least in one experiment (BORAX-6), an inhomogeneous and therefore unrealistic power density due to layer formation in the pool could be avoided. Comparison of the results from this experiment with those of the pure sacrificial material reference experiment (BORAX-7) shows, that the ratio of downward to sideward propagation can be reduced until nearly zero by the insertion of high melting barriers. The insertion of high melting barriers will not equalize downward and sideward penetration as has been tentatively assumed in /1,2/. The transfer of these results to the borax core-catcher seems justified, because, as the other experiments show, these findings do not depend sensitively neither on the local power density distribution nor on the type of structure used as high melting barriers.

Not to surpass certain limits in the liner heat flux, the downward to sideward propagation ratio has to be known for the borax core-catcher. It is known /7-9/ and it has been confirmed by these experiments, that this quantity depends strongly on the liquid to sacrificial material density ratio. For the borax core-catcher, the density ratio (≈ 4) is much higher than the values that could be achieved in the present experiments (≈ 1.7). For this reason and because the propagation ratio may depend on other material properties, it cannot be deduced only from experiments with simulant materials. To achieve a reliable value of this ratio, experiments with the real materials in sufficiently large quantities seem necessary.

Acknowledgements

The authors gratefully acknowledge the help of G. Eck, M. Mösche and E. Simon in performing the experiments. The help of S. Dorner in selecting suitable simulant materials is also much appreciated.

Literature

- /1/ M. Dalle Donne, S. Dorner, G. Fieg, G. Schumacher and H. Werle,
"Development work for Fast Reactor Core-Catchers on the Basis
of Sodium Borates,"
Proc. Int. Meeting Fast Reactor Safety Technology, Seattle,
Aug. 1979, Vol. I, p. 400

- /2/ M. Dalle Donne, S. Dorner and G. Schumacher,
"Development work for a Borax Internal Core-Catcher for a
Gas-Cooled Fast Reactor,"
Nucl. Technology 39 (1978) p. 138

- /3/ M. Dalle Donne, S. Dorner, G. Fieg, G. Schumacher and H. Werle,
"Further work for the GCFR Borax Core-Catcher,"
Specialist Meeting on Gas-Cooled Fast Reactor Safety and
Associated Design Features, Brussels, March 1979

- /4/ G. Fieg and H. Werle,
"Experimental Investigations of Heat Transfer in Pools,"
Proc. Int. Meeting Fast Reactor Safety Technology, Seattle,
Aug. 1979, Vol. I, p. 346

- /5/ G.W. Fieg,
"Heat Transfer from Internally Heated Fluids with Temperature
Dependent Viscosity," to be published in Nucl. Technology

- /6/ L. Baker, Jr., R.E. Faw and F.A. Kulacki,
"Postaccident Heat Removal-Part 1: Heat Transfer within an
Internally Heated, Nonboiling Liquid Layer,"
Nucl. Sci. Eng. 61 (1976) p. 222

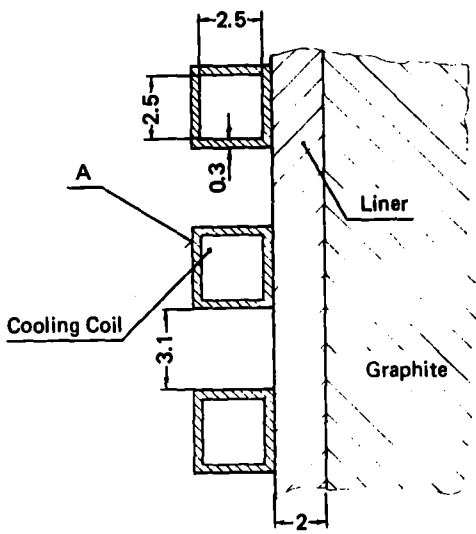
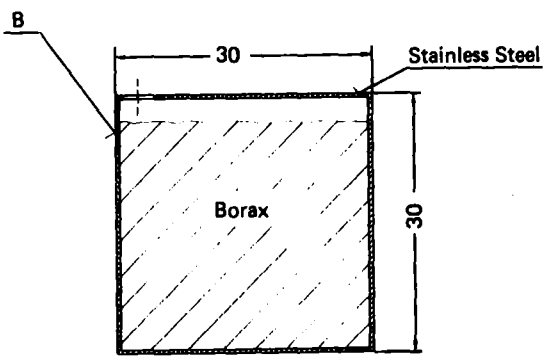
- /7/ R. Farhadich and L. Baker, Jr.,
"Experimental Studies of the Growth of an Internally Heated
Liquid Pool in a Solid Bed,"
Nucl. Sci. Eng. 65 (1978) p. 394

- /8/ R. Farhadich and M.M. Chen,
"Mechanisms Controlling the Downward and Sideward Penetration
of a Hot Liquid into a Solid," to be published.

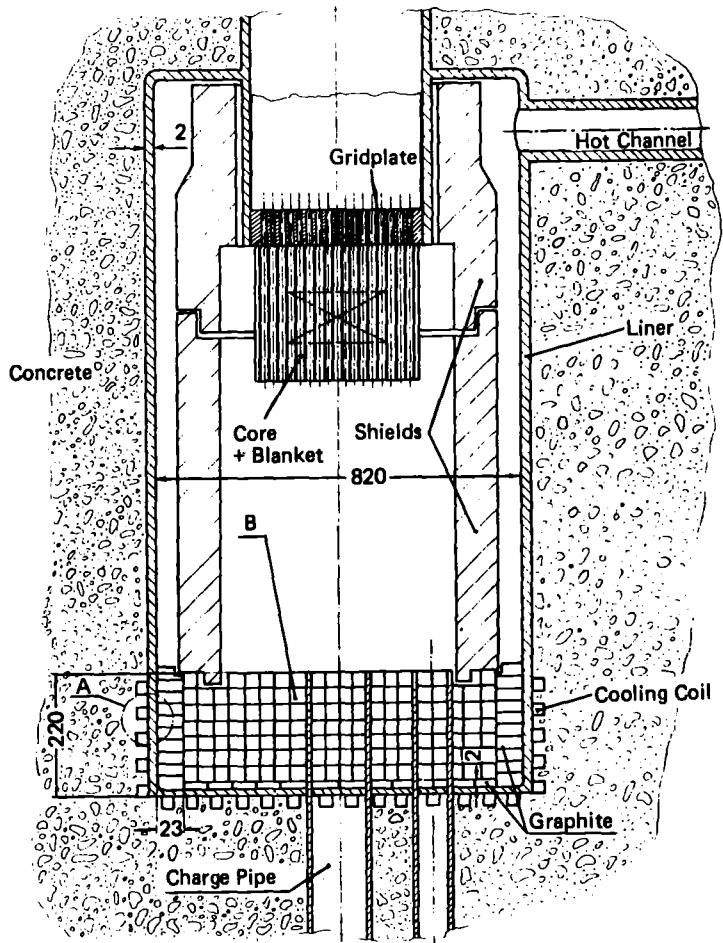
- /9/ G. Fieg and H. Werle,
"Heat Transfer Measurements from Internally Heated Liquids
enclosed in Nonmelting and Melting Boundaries,"
Proc. Third Post-Accident Heat Removal Information Exchange,
Argonne, 1977, ANL-78-10, p. 153

Tab. 1 BORAX-Experiments

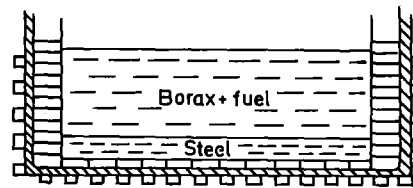
Exp. No.	Date	Overall dimensions/(cm)	Melting material	Wood metal structure	wood metal structure wall thickness	H ₂ O-ZnBr ₂ density ($\frac{g}{cm^3}$), 44°C	Heating	Power (W)
1	Nov. 78	36 * 15 * 10	PEG	Boxes 5*5*5 cm ³	1 mm	1.83	Electr.heated wires	150
2	May 79	"	"		"	1.83	Electrolyc. Mov. electr.-structure	150/200
3	July 79	"	"		0.5 mm	1.19		" "
4	Oct. 79	22 * 17 * 5	"	Cubic structure	0.35 mm	1.83	" "	160/300
5	Nov. 79	"	"	pitch 1 cm	"	1.22	" "	200
6	Dec. 79	"	PEG+H ₂ O-KJ		"	1.81	" "	200
7	Apr. 80	"	PEG	No structure	---	1.83	" Vert. screen electr.	200



Dimensions in Centimetres



Dimensions in Centimetres



after melt down



FIG. 1 CORE-CATCHER LAYOUT INSIDE THE REACTOR IN THE PRESTRESSED CONCRETE REACTOR VESSEL

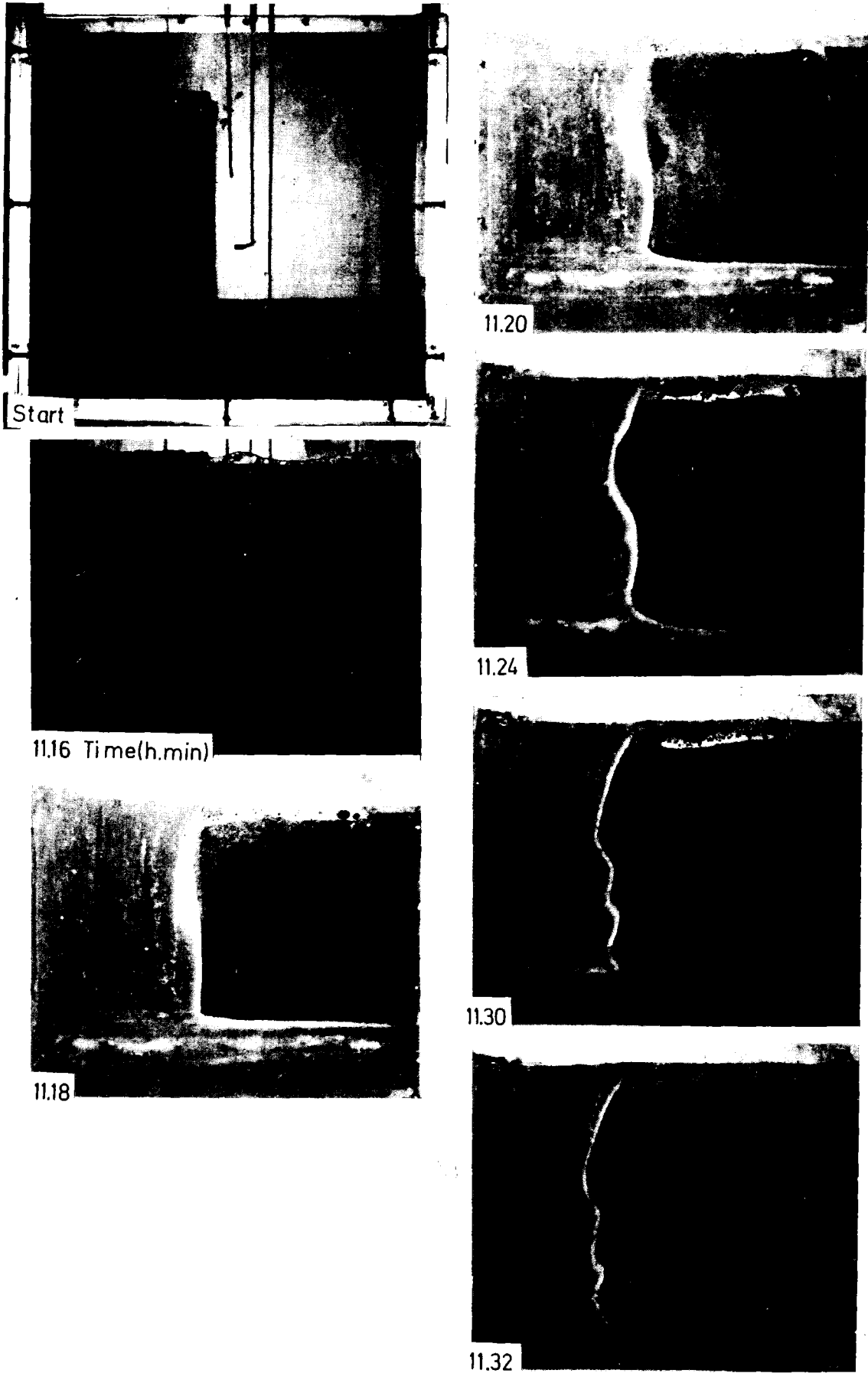


FIG. 2-1 BORAX-7, MELTFRONT PROPAGATION

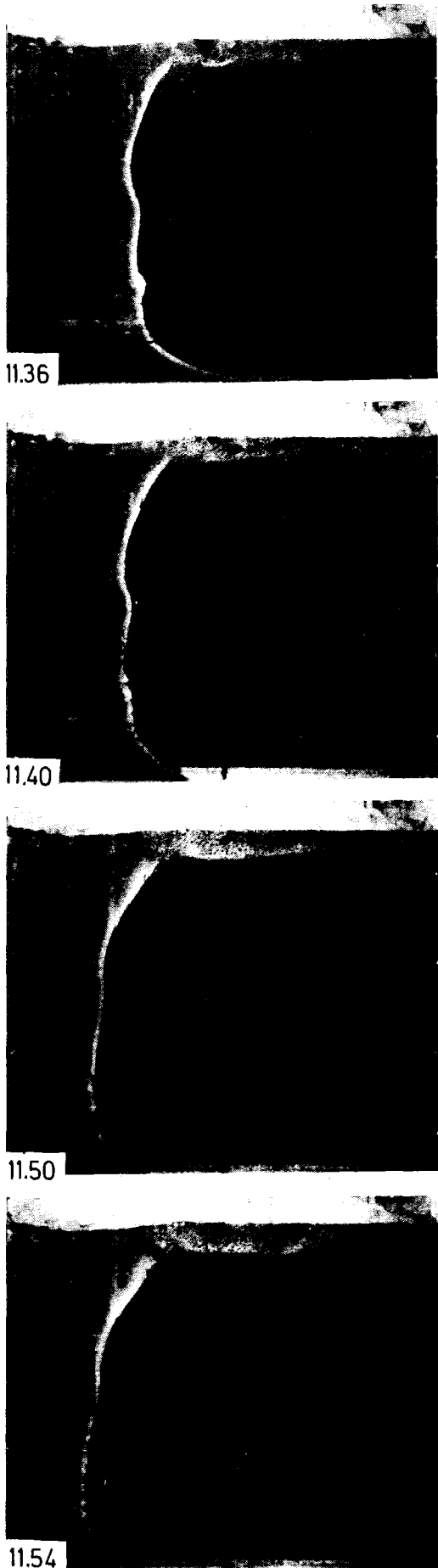


FIG. 2-2 BORAX-7, MELTFRONT PROPAGATION

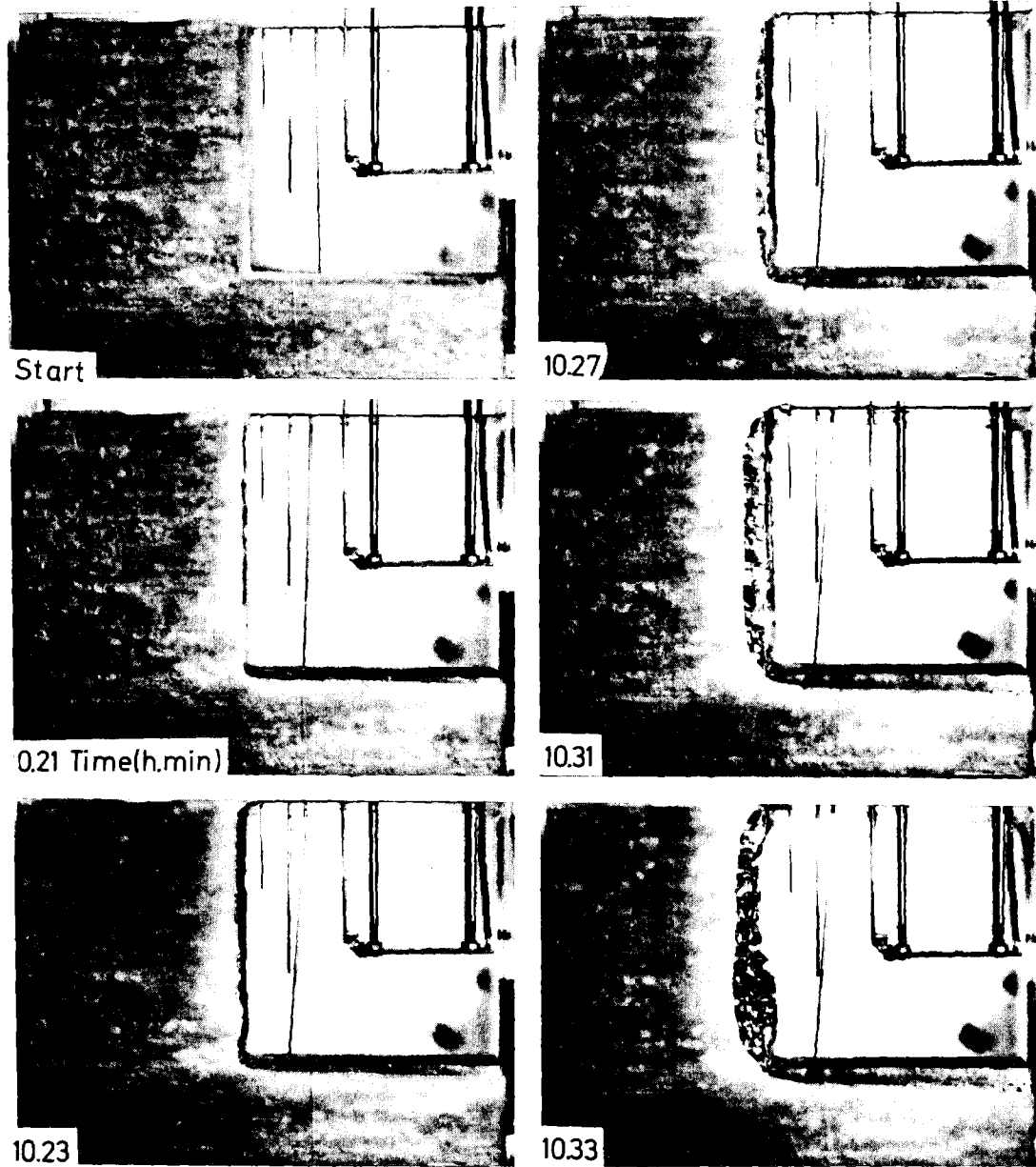
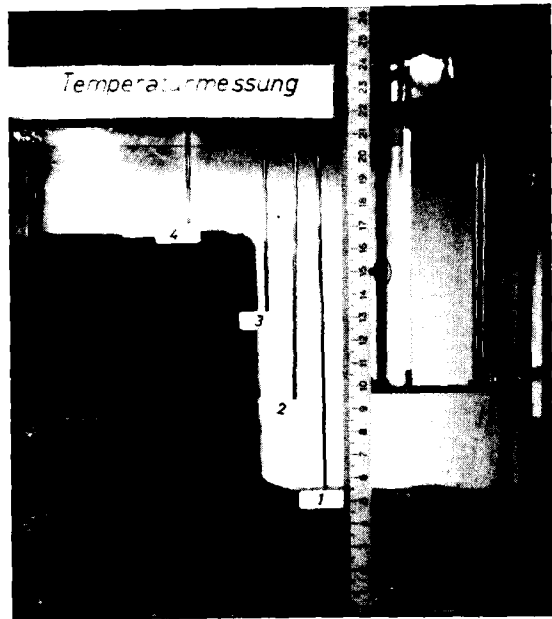


FIG. 3-1 BORAX-4, MELTFRONT PROPAGATION

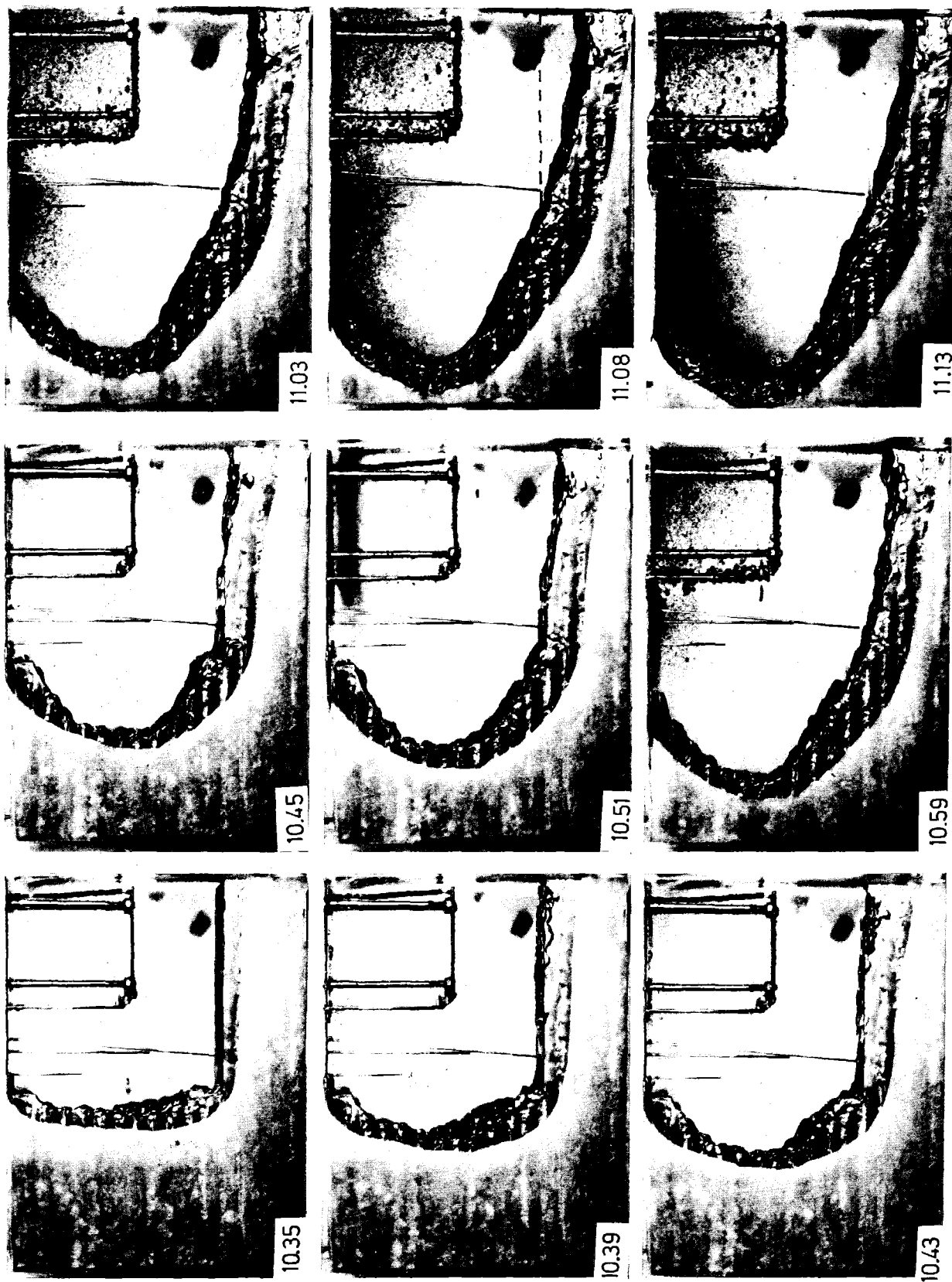


FIG. 3-2 BORAX-4, MELTFRONT PROPAGATION

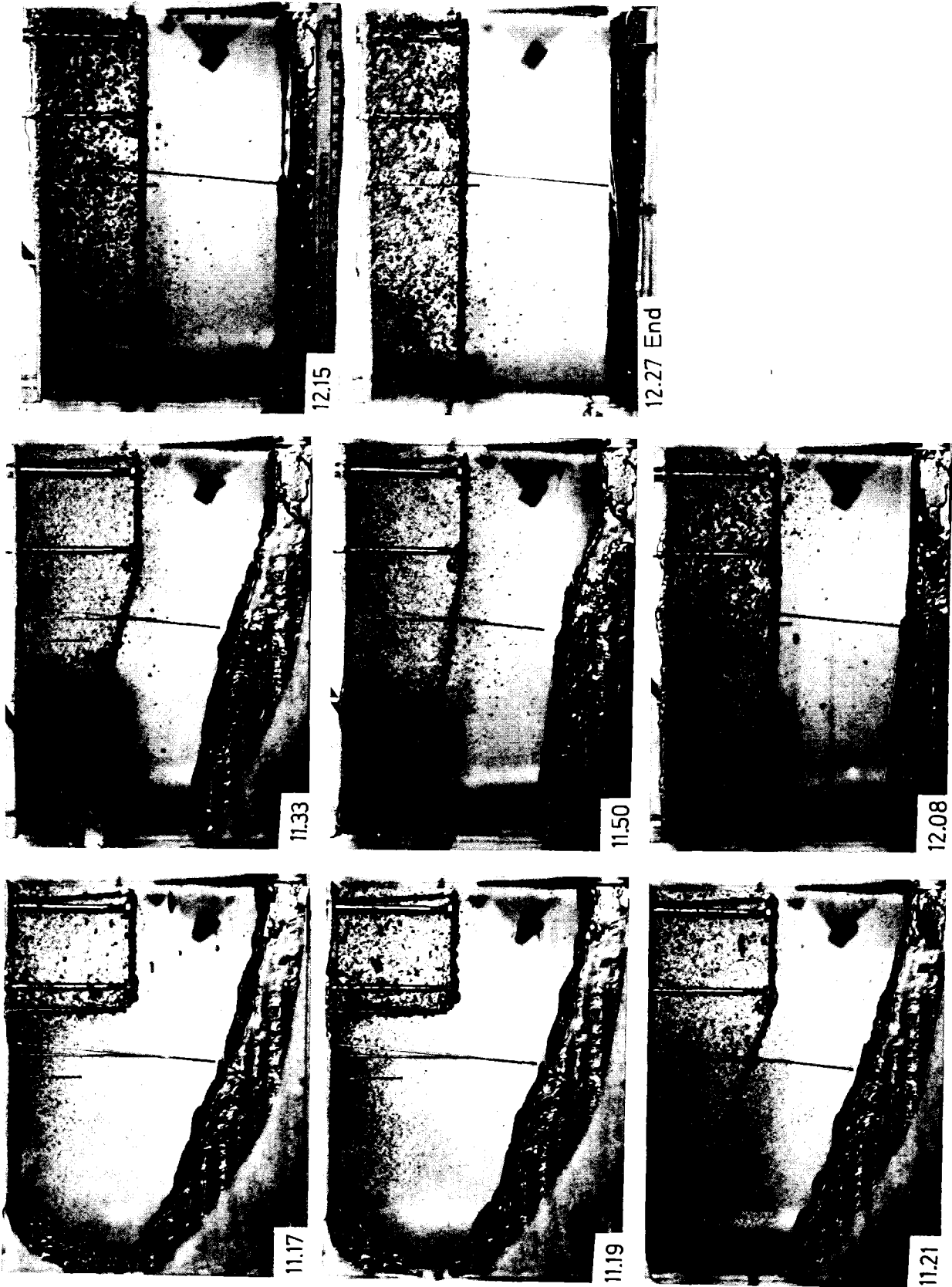
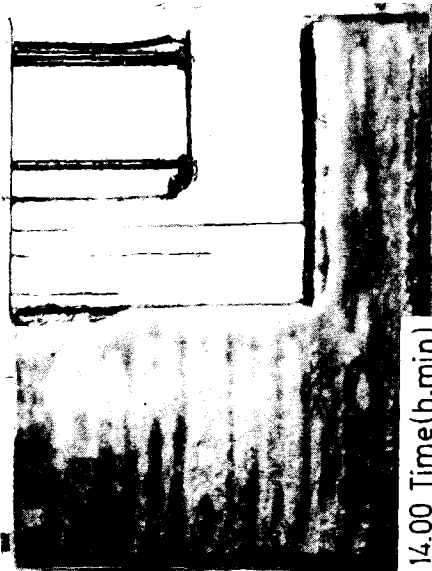
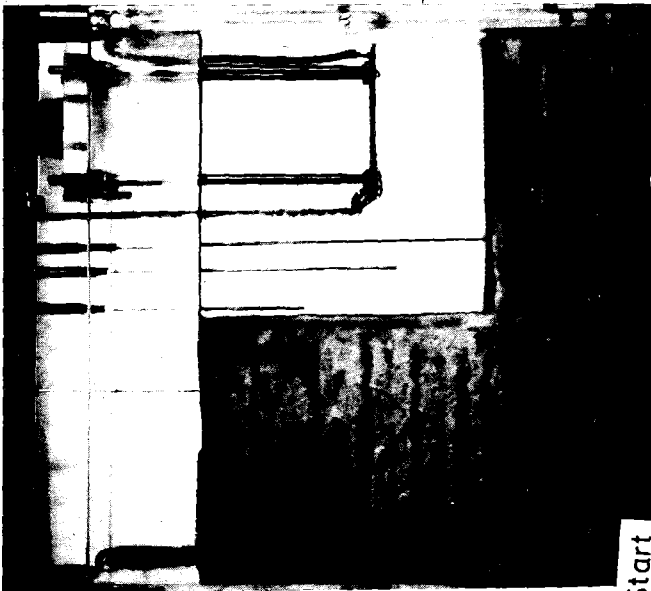
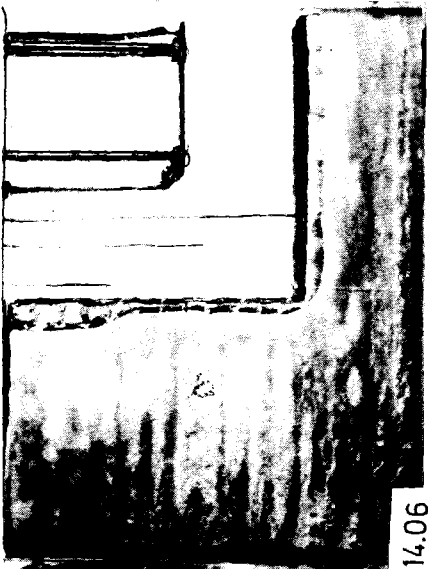


FIG. 3-3 BORAX-4, MELTFRONT PROPAGATION



4-1 BORAX-5, MELTFRONT PROPAGATION

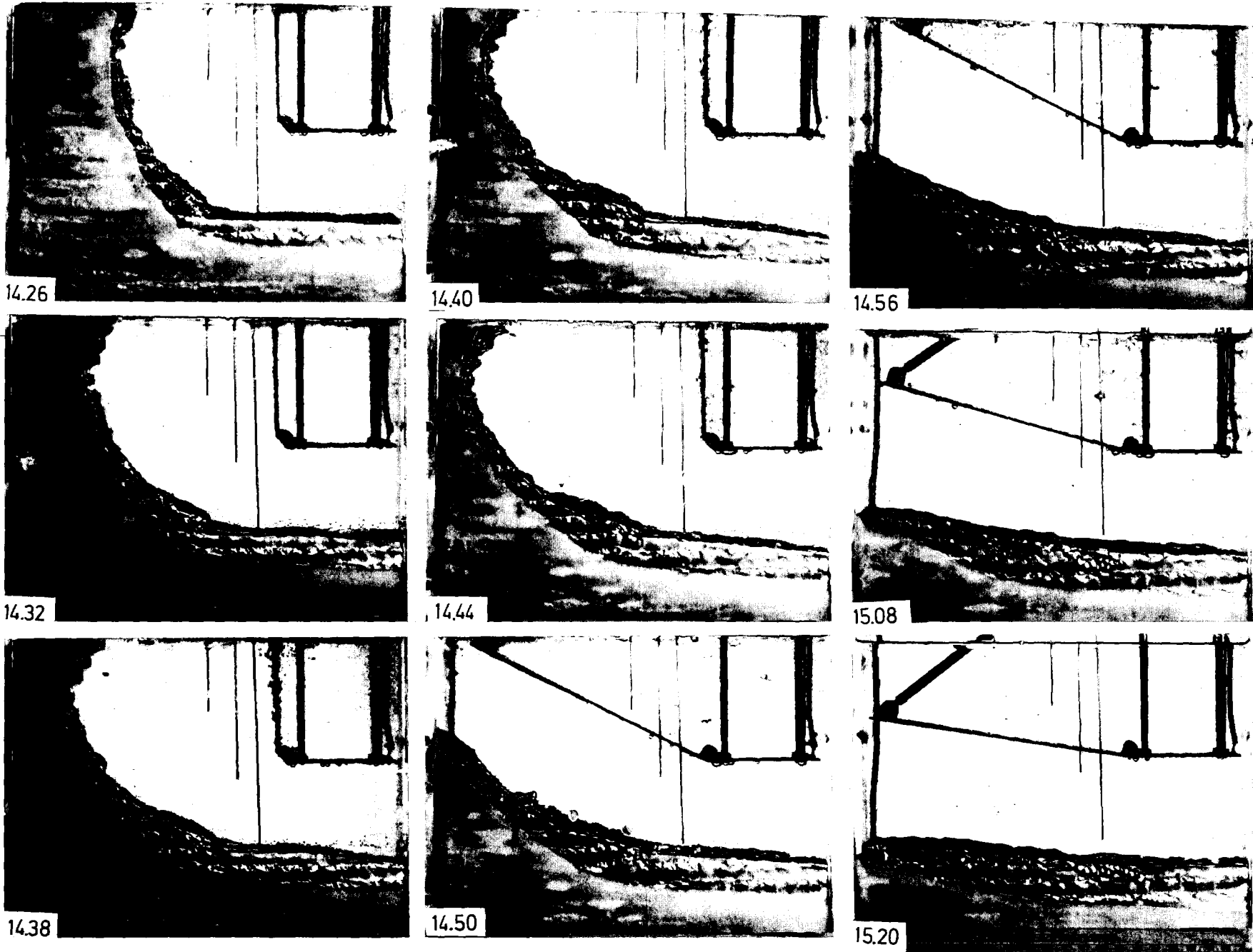


FIG. 4-2 BORAX-5, MELTFRONT PROPAGATION

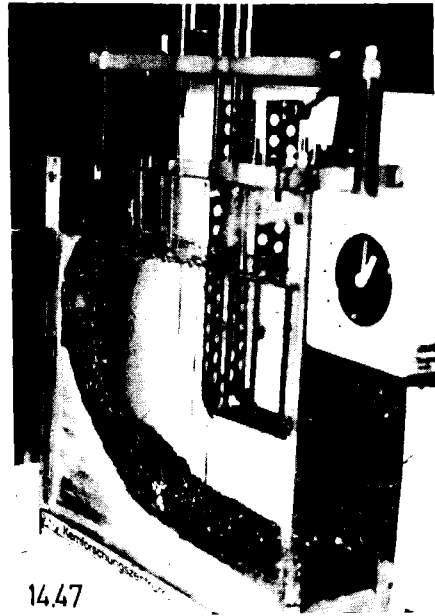
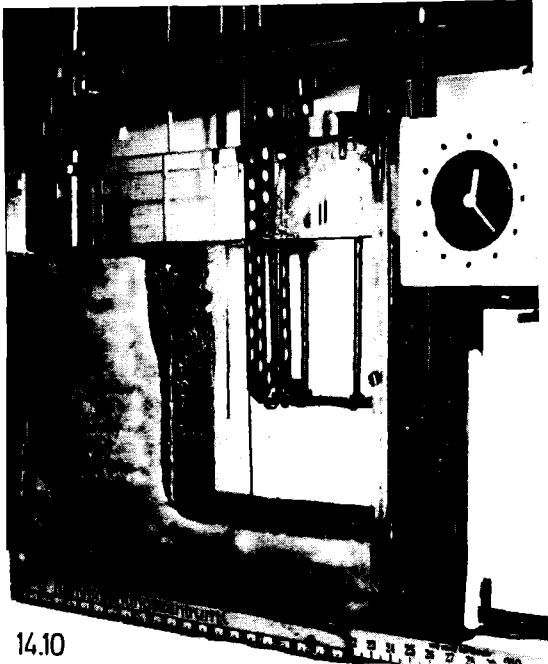


FIG. 4-3 BORAX-5, MELTFRONT PROPAGATION, Special Effects

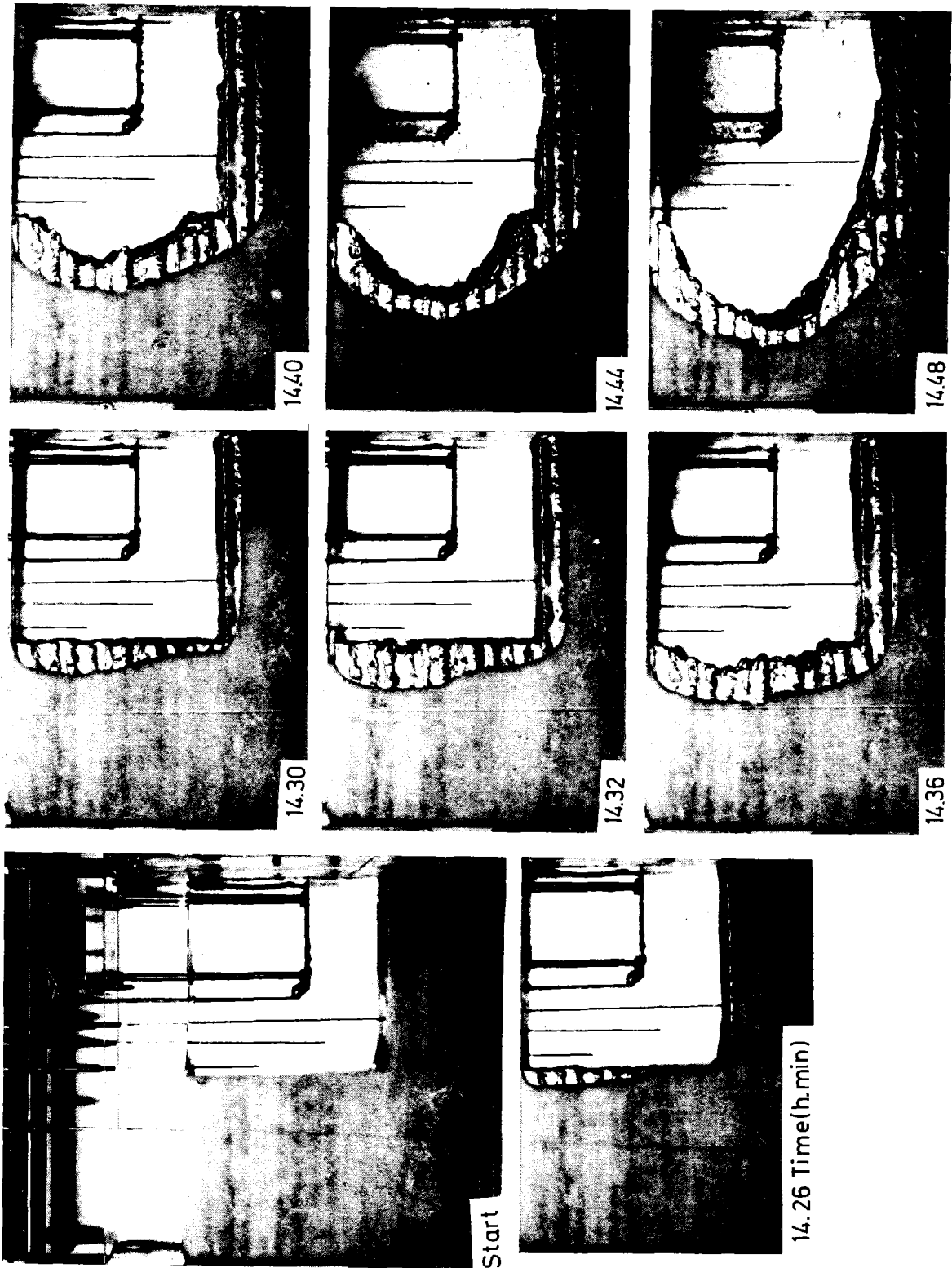


FIG. 5-1 BORAX-6, MELTFRONT PROPAGATION

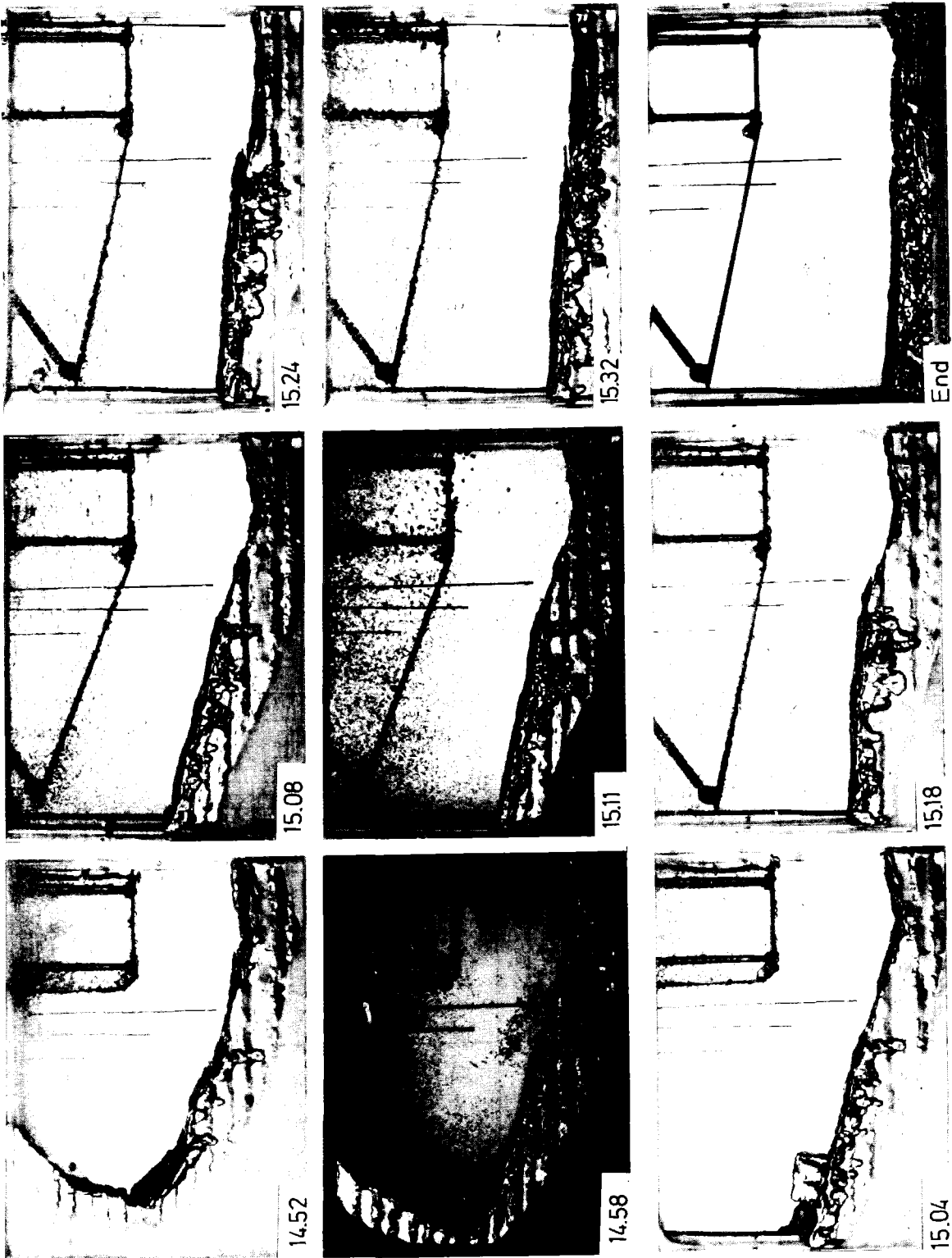


FIG. 5-2 BORAX-6, MELTFRONT PROPAGATION

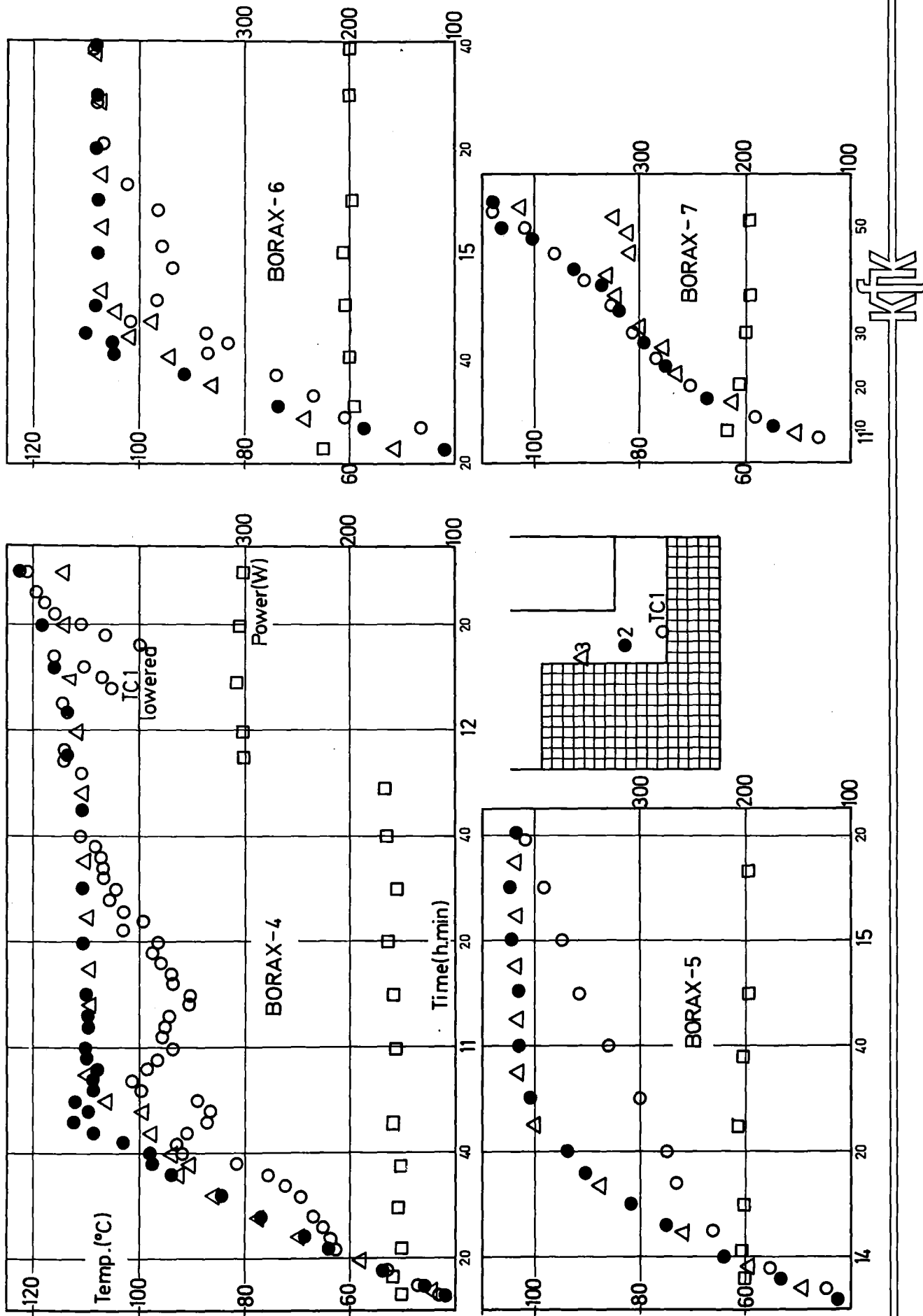


FIG. 6 BORAX-4 TO 7, TEMPERATURES AND POWER VERSUS TIME

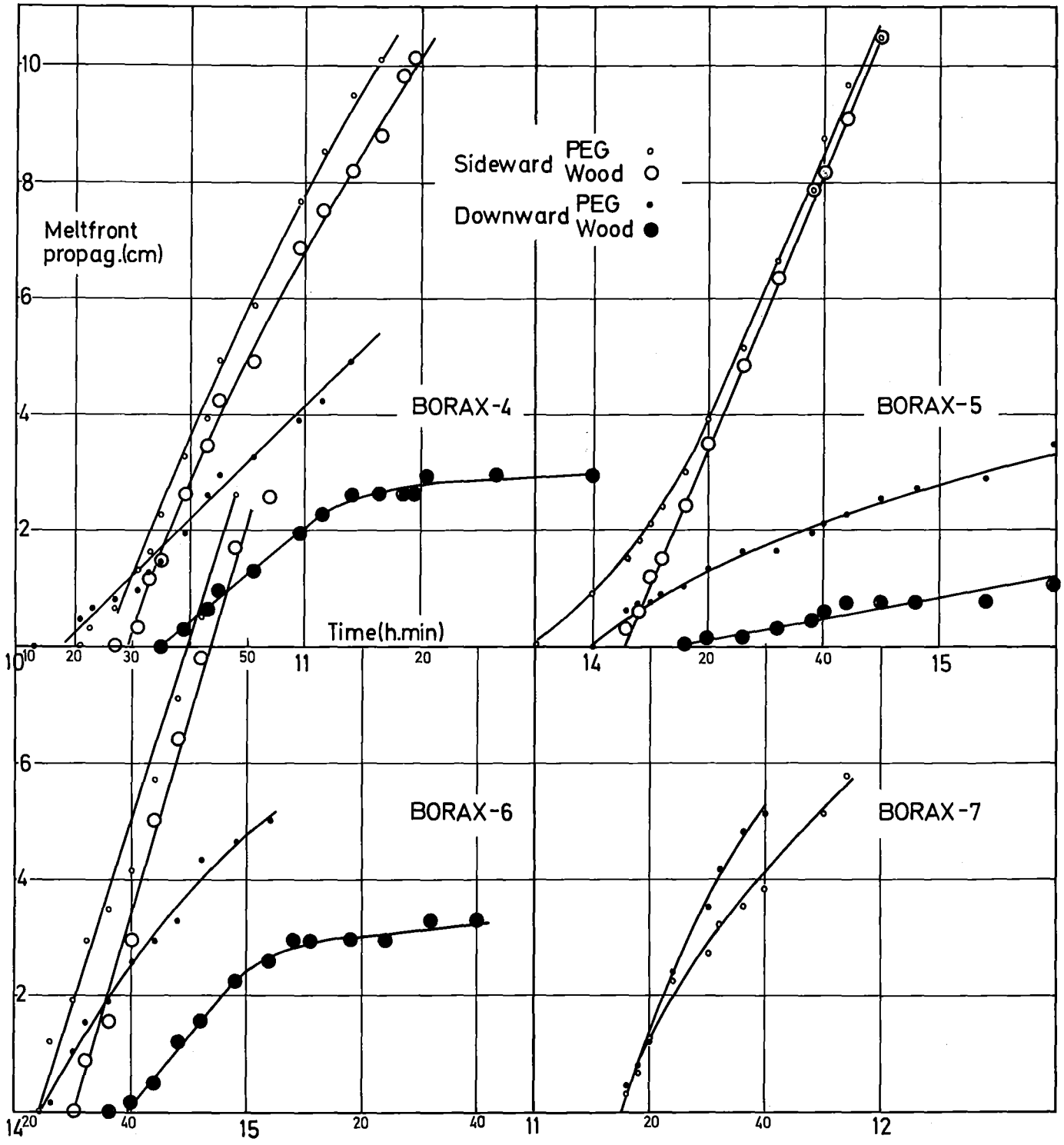
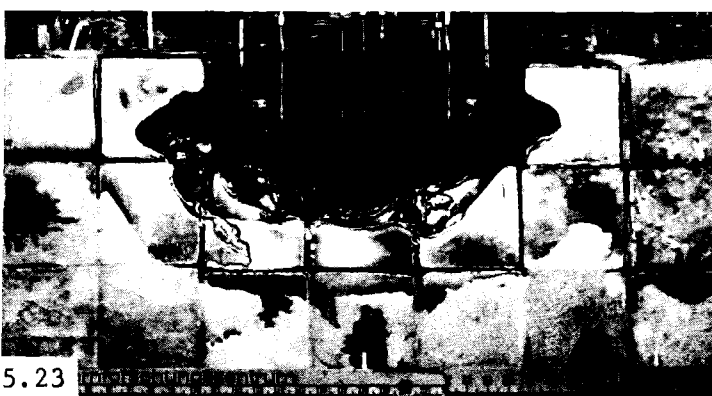
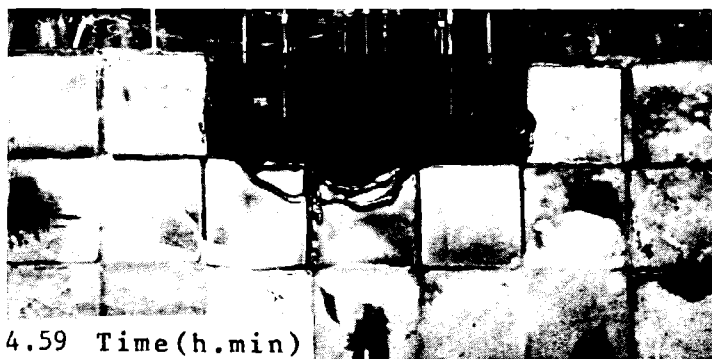
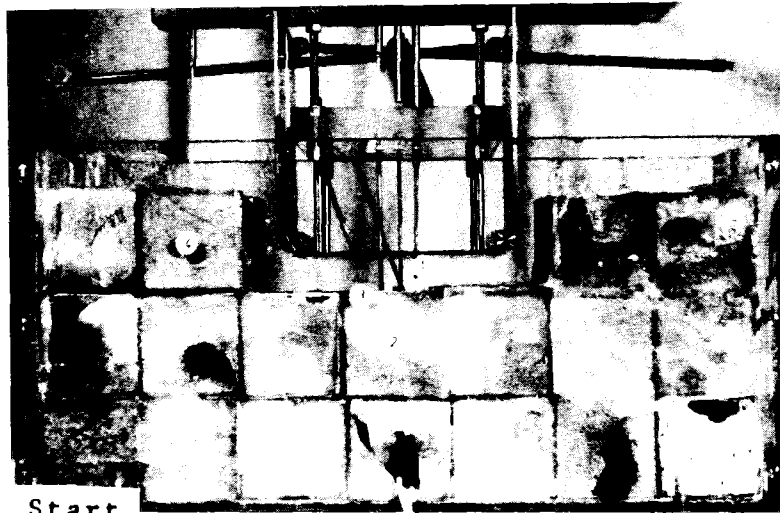


FIG. 7 BORAX-4 TO 7, DOWNWARD AND SIDEWARD MELTFRONT PROPAGATION VERSUS TIME

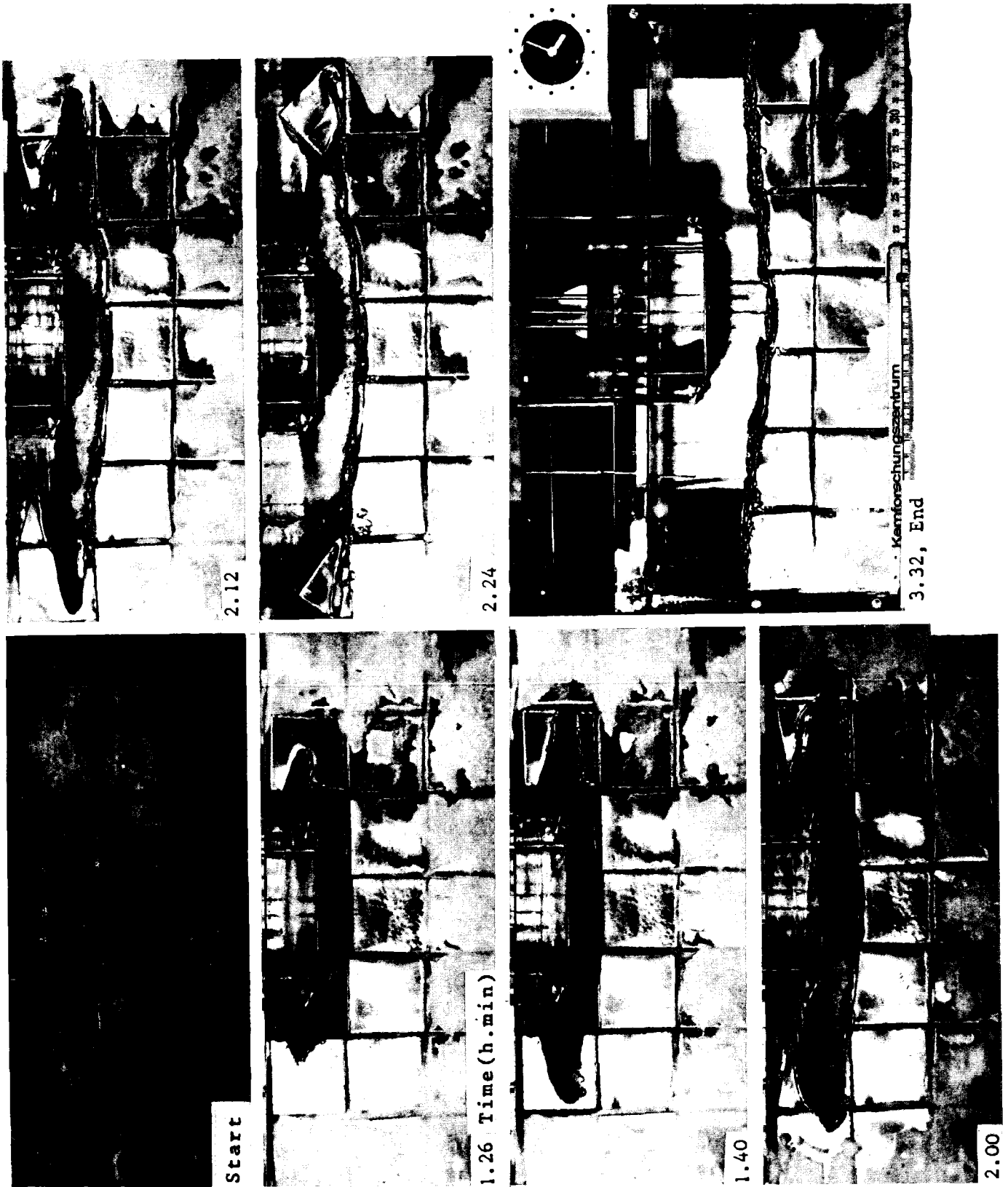


FIG. 8 BORAX-1, MELTFRONT PROPAGATION



KFK

FIG. 9 BORAX-2, MELTFRONT PROPAGATION



KfK

FIG. 10 BORAX-3, MELTFRONT PROPAGATION

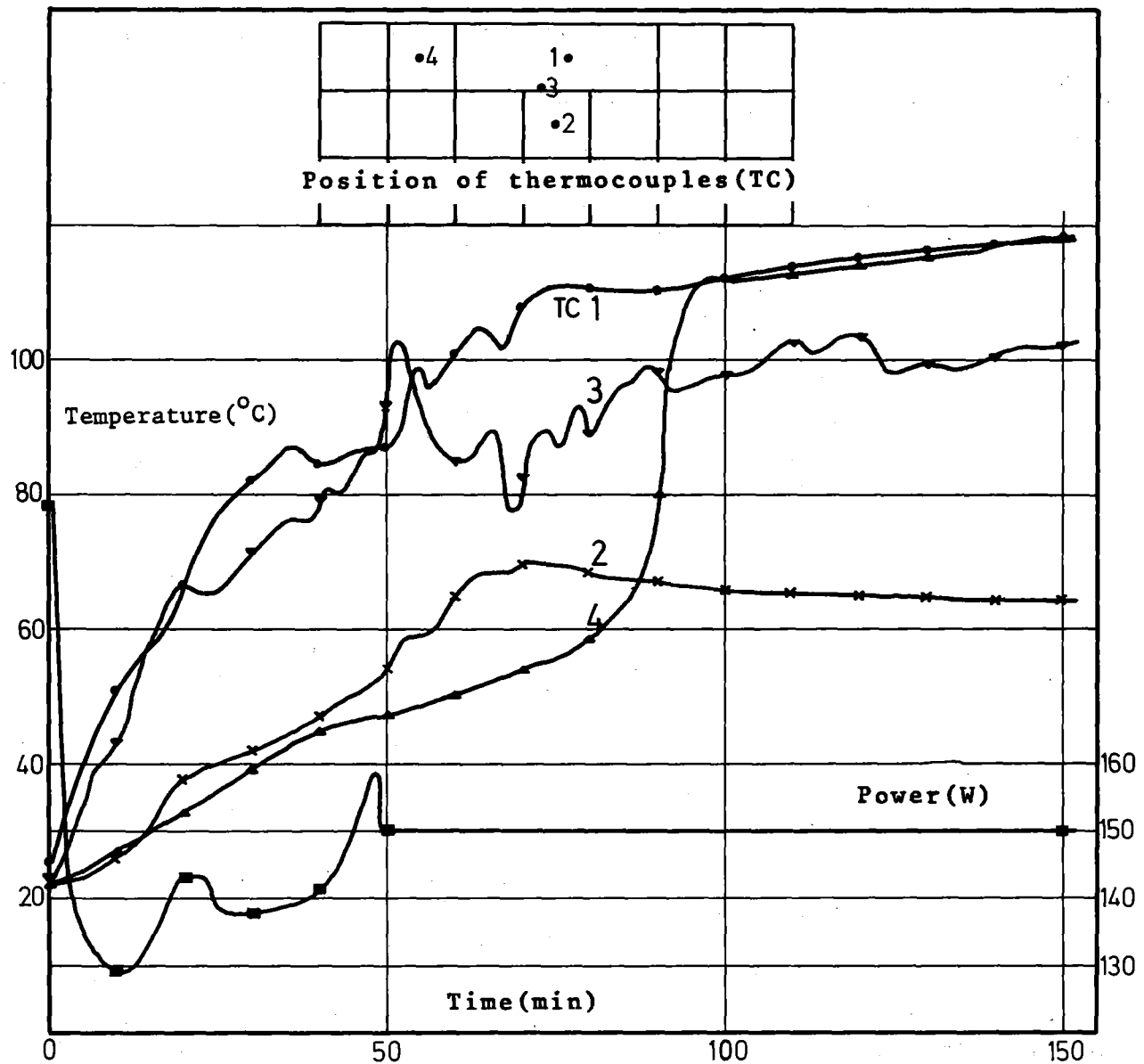


FIG. 11 BORAX-1, TEMPERATURE AND POWER VERSUS TIME



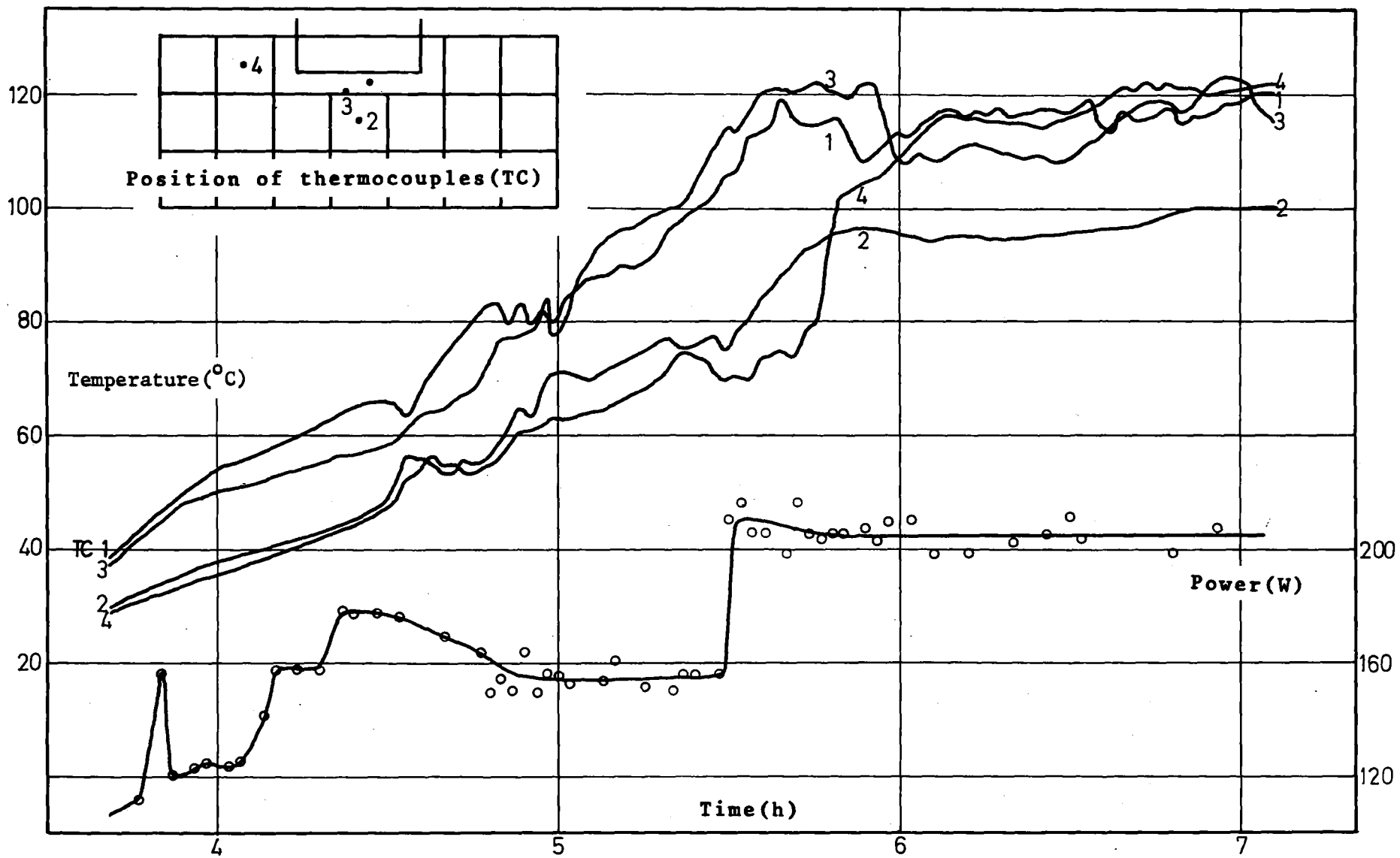


FIG. 12 BORAX-2, TEMPERATURE AND POWER VERSUS TIME

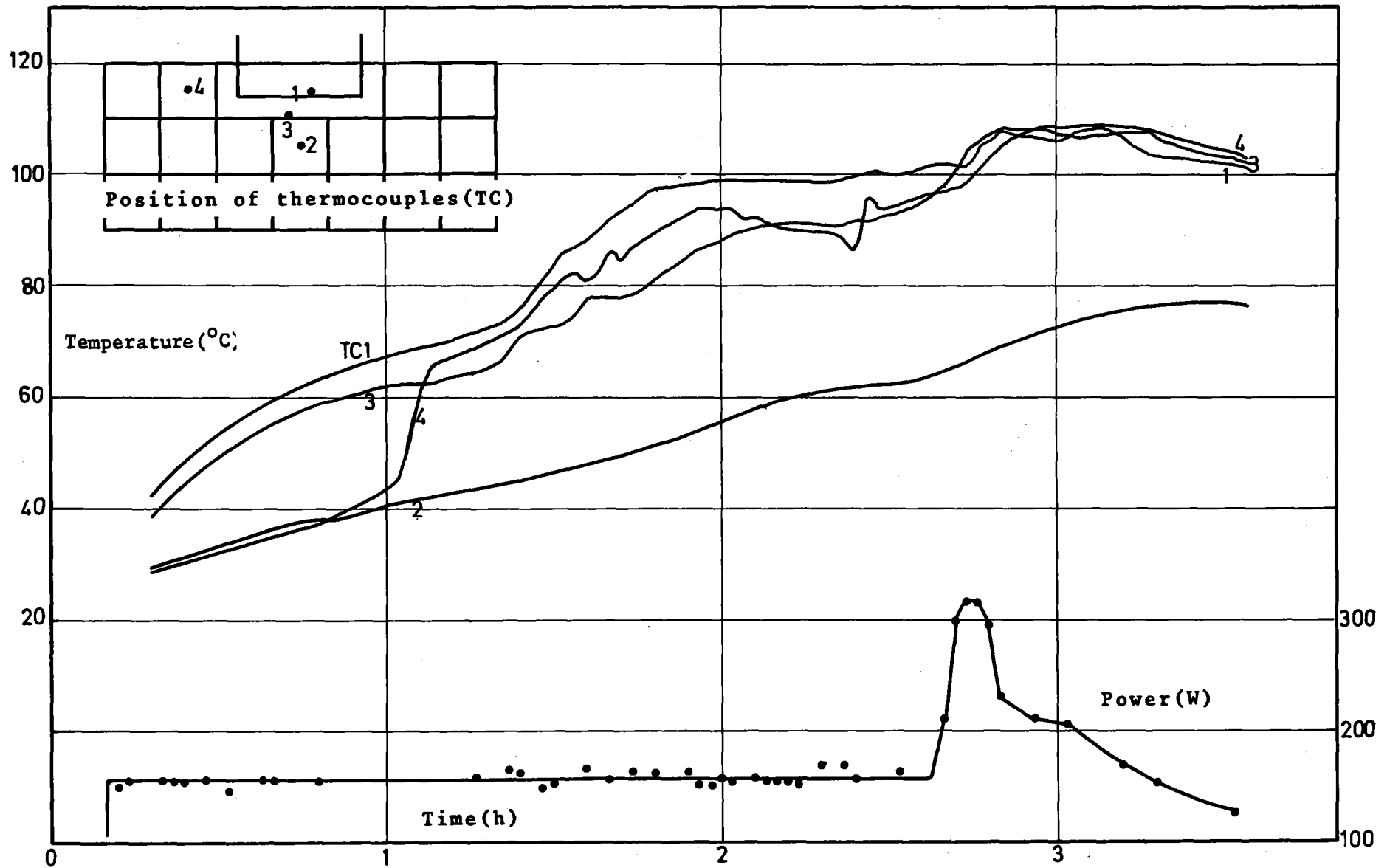


FIG. 13 BORAX-3, TEMPERATURE AND POWER VERSUS TIME

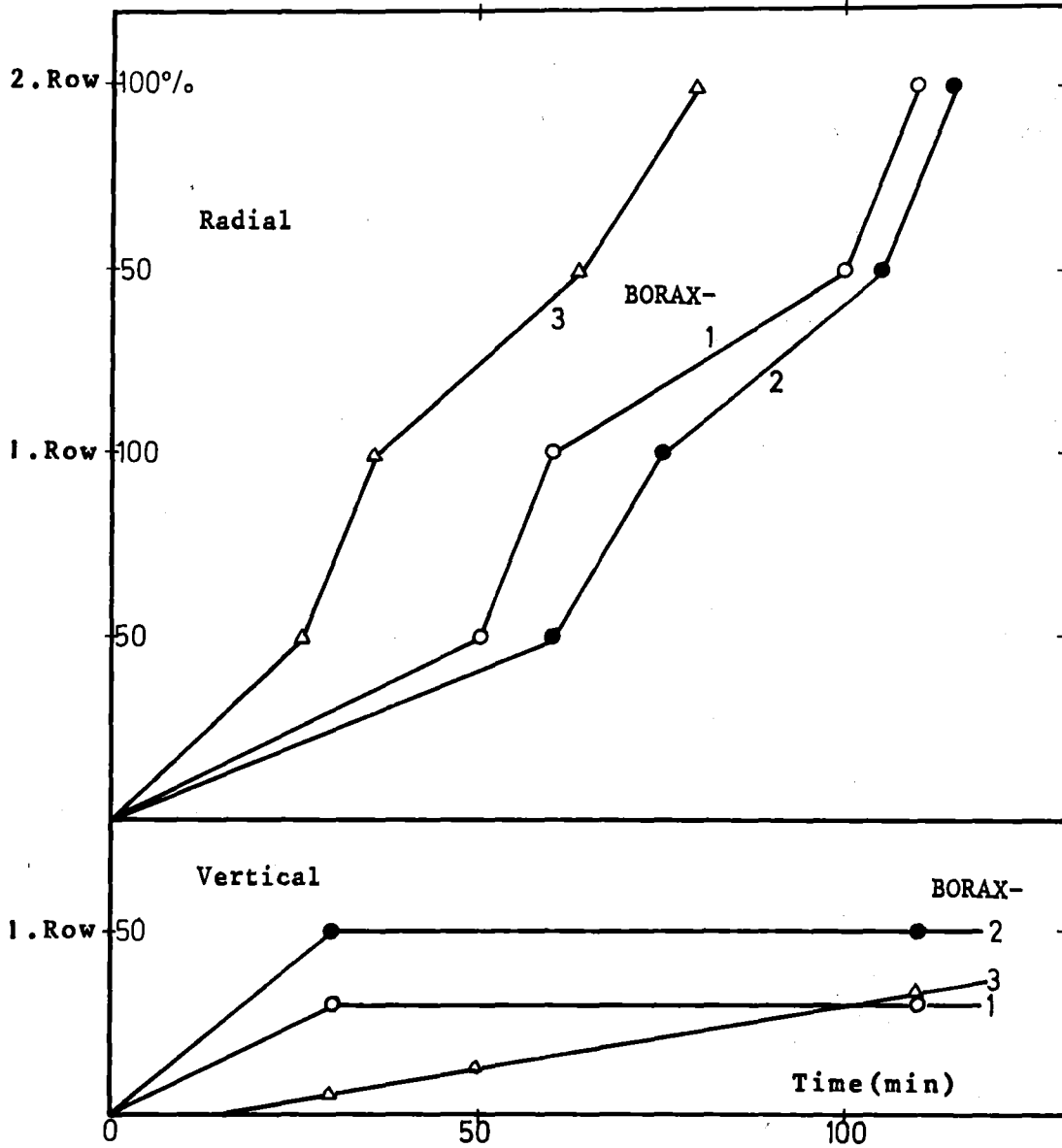
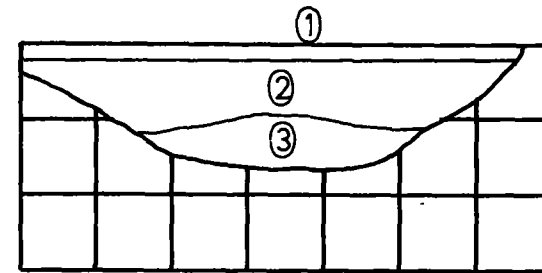
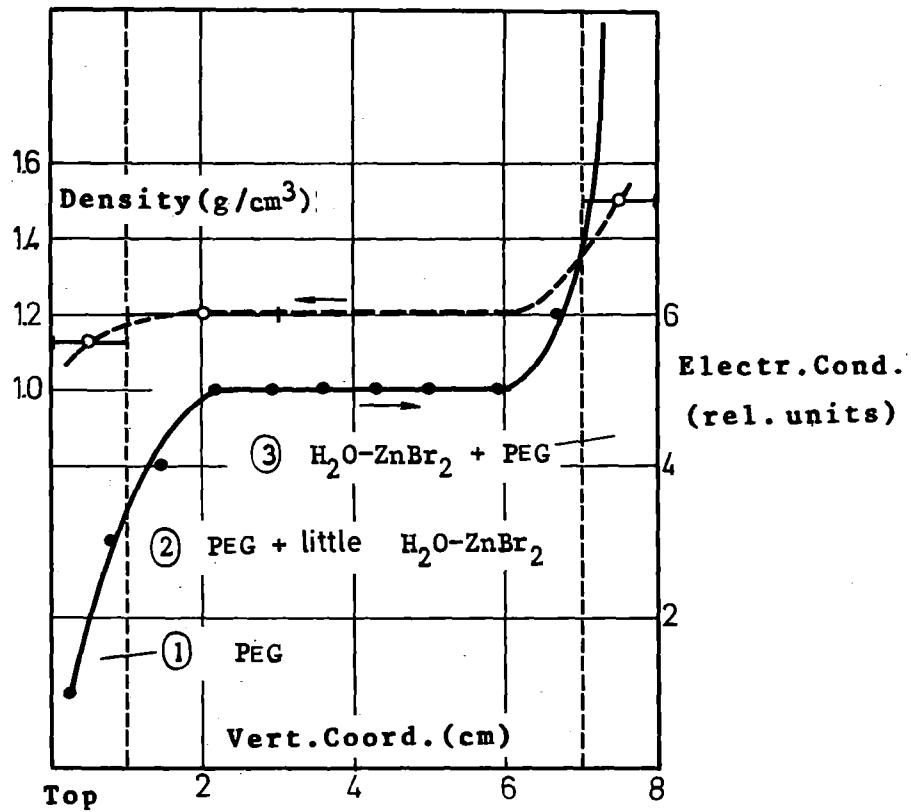


FIG. 14 BORAX-1 TO 3, DOWNWARD AND SIDEWARD WOOD METAL STRUCTURE MELTFRONT PROPAGATION VERSUS TIME



- ① PEG
- ② PEG + little H₂O-ZnBr₂
- ③ H₂O-ZnBr₂ + PEG



FIG. 15 BORAX-2, LAYER FORMATION IN POOL